TU Delft

Delft University of Technology

Document Version
Final published version

Citation (APA)
Corbeski, I., Horn, V., van der Valk, R. A., le Paige, U., Dame, R. T., & van Ingen, H. (2024). Microscale Thermophoresis Analysis of Chromatin Interactions. In R. T. Dame (Ed.), *Bacterial Chromatin : Methods and Protocols* (pp. 357-379). (Methods in Molecular Biology; Vol. 2819). Springer. https://doi.org/10.1007/978-1-0716-3930-6_17

Important note
To cite this publication, please use the final published version (if applicable).
Please check the document version above.

Copyright
In case the licence states “Dutch Copyright Act (Article 25fa)”, this publication was made available Green Open Access via the TU Delft Institutional Repository pursuant to Dutch Copyright Act (Article 25fa, the Taverne amendment). This provision does not affect copyright ownership.
Unless copyright is transferred by contract or statute, it remains with the copyright holder.

Sharing and reuse
Other than for strictly personal use, it is not permitted to download, forward or distribute the text or part of it, without the consent of the author(s) and/or copyright holder(s), unless the work is under an open content license such as Creative Commons.

Takedown policy
Please contact us and provide details if you believe this document breaches copyrights.
We will remove access to the work immediately and investigate your claim.

This work is downloaded from Delft University of Technology.

Green Open Access added to TU Delft Institutional Repository

'You share, we take care!' - Taverne project

https://www.openaccess.nl/en/you-share-we-take-care

Otherwise as indicated in the copyright section: the publisher is the copyright holder of this work and the author uses the Dutch legislation to make this work public.

Chapter 17

Microscale Thermophoresis Analysis of Chromatin Interactions

Ivan Corbeski, Velten Horn, Ramon A. van der Valk, Ulric le Paige, Remus T. Dame, and Hugo van Ingen

Abstract

Architectural DNA-binding proteins are key to the organization and compaction of genomic DNA inside cells. The activity of architectural proteins is often subject to further modulation and regulation through the interaction with a diverse array of other protein factors. Detailed knowledge on the binding modes involved is crucial for our understanding of how these protein-protein and protein-DNA interactions shape the functional landscape of chromatin in all kingdoms of life: bacteria, archaea, and eukarya.

Microscale thermophoresis (MST) is a biophysical technique for the study of biomolecular interactions. It has seen increasing application in recent years thanks to its solution-based nature, rapid application, modest sample demand, and the sensitivity of the thermophoresis effect to binding events.

Here, we describe the use of MST in the study of chromatin interactions. The emphasis lies on the wide range of ways in which these experiments are set up and the diverse types of information they reveal. These aspects are illustrated with four very different systems: the sequence-dependent DNA compaction by architectural protein HMfB, the sequential binding of core histone complexes to histone chaperone APLF, the impact of the nucleosomal context on the recognition of histone modifications, and the binding of a viral peptide to the nucleosome. Special emphasis is given to the key steps in the design, execution, and analysis of MST experiments in the context of the provided examples.

Key words MST, Chromatin, Nucleosome, Histone, Chaperone, HMf, DNA, Peptide, IDP, Binding affinity

1 Introduction

Biophysical characterization of functional chromatin interactions has typically relied thus far on the electrophoretic mobility shift assay (EMSA) for protein-DNA interactions as well as on common biophysical techniques such as surface plasmon resonance (SPR) spectroscopy, isothermal titration calorimetry (ITC), and nuclear magnetic resonance (NMR) spectroscopy [1–3]. Thorough characterization of binding modes and affinities is often a critical step preceding structural and functional studies. This calls for a fast and

Remus T. Dame (ed.), *Bacterial Chromatin: Methods and Protocols*, Methods in Molecular Biology, vol. 2819,
https://doi.org/10.1007/978-1-0716-3930-6_17,
© The Author(s), under exclusive license to Springer Science+Business Media, LLC, part of Springer Nature 2024

flexible technique that can characterize interactions in solution with reasonable throughput and modest sample demands. Microscale thermophoresis (MST) fulfills these criteria and thus provides an efficient option for the analysis of biomolecular interactions.

1.1 Microscale Thermophoresis (MST)

Analogous to electrophoresis where charged molecules move in response to an electric field, thermophoresis is the flow or directed movement of molecules along a temperature gradient [4]. Technological advances have made it possible to use small temperature gradients (typically 2–6 °C) and detect the resulting micrometer-scale movements, allowing the application in molecular biology as microscale thermophoresis (MST) [5].

MST typically requires chemical fluorescent labeling of the molecule of interest for high-sensitivity detection. However, fluorescent proteins used as common protein tags (e.g., GFP, YFP, mCherry) can be used, too [6], and the intrinsic tryptophan fluorescence of proteins can be exploited as well to gain valuable binding and mechanistic information [7].

Samples are loaded into glass capillaries of which a specific spot is heated by an infrared laser (*see* Fig. 1a). The resulting temperature gradient causes thermophoresis of the labeled molecule, typically away from the heated spot, which is observed through a decrease in fluorescence in the heated region (*see* Fig. 1b). Since thermophoresis is sensitive to molecular size, charge, and hydration shell [8], changes in these properties due to a binding partner will cause changes in thermophoresis of the fluorescent molecule.

For interaction analysis, MST curves are recorded as titration series with increasing amounts of ligand and normalized with respect to their initial equilibrium fluorescence (F_{norm}) (Fig. 1b). A binding curve is extracted by plotting the F_{norm} values from the end of the laser-on period (phase IV, Fig. 1b), which captures binding-induced changes both in thermophoresis and in the intrinsic temperature-related intensity change (TRIC) of the fluorophore (indicated as "thermophoresis + T-jump" in Fig. 1b). Both effects "thermophoresis" and "T-jump" can also be analyzed separately. Since the observed F_{norm} values are the population-weighted averages of the unbound and bound molecules, standard methods can be used to fit the binding curve and extract the binding affinity.

MST can be performed in virtually every buffer [9], as well as with unpurified proteins in cell lysates [10]. Other characteristics such as thermodynamic properties, binding stoichiometry, and enzyme kinetics can be extracted with customized experimental designs [11].

1.2 MST of Chromatin Systems

The study of chromatin function is strongly connected to protein-DNA and protein-protein interactions that modulate the chromatin state. An increasing number of studies have employed MST to investigate binding events in chromatin-related systems (*see*, for

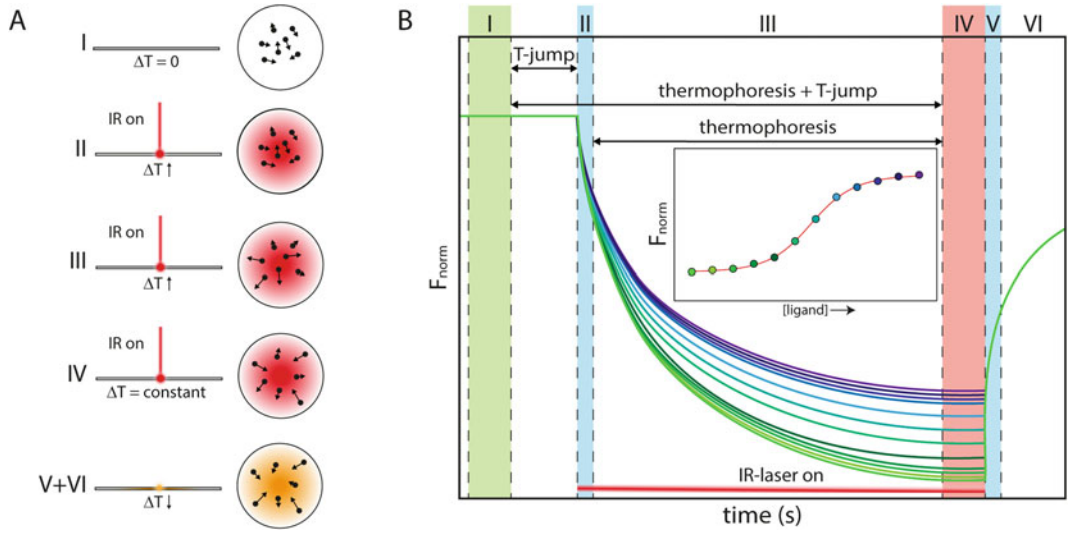

Fig. 1 Principle of MST. Schematic depiction of the MST experiment (**a**) and MST time traces (**b**). In (**a**), the capillaries (left) and particles in a cross section thereof (right) during different stages of the experiment (phases I–VI) are shown. Starting from equilibrium (phase I), infrared (IR) laser irradiation is started (phase II), causing particles to move out or into the heated volume ("thermophoresis," phase III). When thermophoresis is counterbalanced by mass diffusion, a steady state is reached (phase IV). When the IR laser is switched off, the particle concentration re-equilibrates (phases V + VI). In (**b**), a titration series is shown, relative ligand concentration and plotted binding curve indicated in the inset. Each sample is characterized by a distinct thermophoresis curve. The rapid change in normalized fluorescence in phases II and V is caused by the fluorophore's temperature-related intensity change (TRIC) in fluorescence ("T-jump"). Binding curves can be extracted by plotting F_{norm} values for regions "T-jump" (I vs. II), "thermophoresis + T-jump" (I vs. IV), or "thermophoresis" (II vs. IV)

instance, Refs. [12–16]), and some of the earliest examples have been included in reviews [1, 17–19]. A variety of labeling strategies have emerged, in particular for the study of protein-nucleosome interactions. Fluorescent nucleosomes have been constructed using Cy5-labeled DNA [19] or Alexa Fluor 647-labeled histone H3 [20]. Furthermore, MST has been used to derive insights into protein-binding mechanisms, e.g., demonstration of cooperative binding [21] or determination of binding sites from a comparison of different deletion mutants [22].

Here, we describe in detail the use of MST to study chromatin interactions and put particular emphasis on the step-by-step optimization of experimental conditions. We present examples on the interaction of architectural proteins with other proteins and DNA, which illustrate the information MST can provide on the binding mechanism, the sensitivity of the thermophoresis, and the merits of custom data analysis. Furthermore, we provide first-hand reports on assay issues that can be observed for various chromatin-related samples and strategies to detect and overcome them.

The described examples demonstrate that MST can produce reproducible binding data for chromatin-associated complexes in a convenient manner, using small amounts of materials and minimalistic labeling approaches that do not interfere with the binding reaction. Furthermore, due to its fluorescence-detection-based setup, the sensitivity of the experiment might reveal in some cases additional binding modes with important functional implications which would otherwise remain hidden when using other techniques.

2 Materials

2.1 Fluorescent Labeling

1. Monolith NT Protein Labeling Kit RED/GREEN/BLUE (NanoTemper Technologies, hereafter referred to as "manufacturer"), either NT-647-NHS or NT-647-MALEIMIDE, which react with solvent-exposed primary amine or sulfhydryl groups, respectively, to form dye-protein conjugates (*see* **Note 1**).
2. Variable-speed benchtop microcentrifuge.
3. 0.2–2 mL microcentrifuge tubes.
4. 10 mL assay buffer (*see* **Note 2**).
5. Dimethylsulfoxide (DMSO).
6. Heating block for microcentrifuge tubes capable of reaching 95 °C.

2.2 MST Materials, Equipment, and Software

We limit the description of the method to the Monolith NT.115 instrument, the NT Control, and NT Analysis software from NanoTemper Technologies (Munich, Germany). Instruments with higher fluorescence sensitivity (for picomolar affinity determination), a setup to excite and detect intrinsic tryptophan fluorescence, a high-throughput automated screening setup, and a setup to detect spectral shifts are also available with updated control and analysis software packages.

The setup used here is as follows:

1. MST instrument Monolith NT.115 equipped with "Red" channel (NanoTemper Technologies).
2. Capillaries: NT.115 standard, hydrophobic, hydrophilic (*see* **Note 3**), or premium-treated capillaries, or the Monolith Explorer Kit-Mission to Mars (NanoTemper Technologies).
3. Personal computer with dedicated NT Control and Affinity Analysis software (version 1.5.41). Alternatively, in-house analysis scripts can be used, e.g., made with MATLAB 2017a (the MathWorks, Inc.) software used here (scripts available upon request).

4. Small-volume reaction tubes (e.g., as found in the labeling kit or 200 μL PCR tubes).
5. Calibrated pipettes in the range 2–1000 μL.
6. NanoDrop Spectrophotometer (Thermo Scientific).
7. Aluminum foil.

2.3 Stock Solutions

The following stock solutions are useful when performing MST experiments (*see* **Note 4**):

1. At least 100 μL of 20 μM of biomolecule to be labeled (*see* **Note 5**).
2. 100 μL of biomolecule to be titrated with a concentration 100 times the expected dissociation constant (*see* **Note 5**).
3. 10 mL of assay buffer (*see* also **Note 2**).
4. 10–100 mg/mL bovine serum albumin (BSA).
5. 5–10% Tween-20.
6. 4 M NaCl.

3 Methods

3.1 Design of MST Experiment: Choice of Fluorescent Labeling

The MST experiment can be performed with either of the interaction partners fluorescently labeled (*see* **Note 6**). Proteins and peptides can be labeled either with the manufacturer's labeling kits or with other widely available fluorophores and coupling strategies (*see* also **Note 1**). DNA molecules are readily labeled using custom oligo synthesis with commercially available labeled nucleotides or using modifications of the termini for coupling with dyes. For the applications described below, proteins were labeled using the manufacturer's supplied labeling kits as detailed in Subheading 3.1.1; preparation of DNA is described in Subheading 3.1.2.

3.1.1 Protein Labeling

The manufacturer's protein labeling kit (NanoTemper Technologies) provides the fluorescent dye, labeling buffer, and purification materials. Labeling and purification of proteins with molecular weight (MW) > 5 kDa can be performed in less than 1 h. The provided dye (NT-647) reacts with either solvent-exposed primary amines (protein N-terminus, lysine sidechains; dye NT-647-NHS) or sulfhydryl groups (cysteine sidechains; dye NT-647-MALEIMIDE) to form dye-protein conjugates. Both, the N-hydroxysuccinimide (NHS)-ester and the maleimide chemistry of the labeling reaction require that the labeling buffer does not contain imidazole, primary amines, or sulfhydryls since these substances significantly reduce protein labeling efficiency (*see* **Note 7**).

For the production of 200 μL of 10 μM labeled protein:

1. If the protein stock solution does not contain interfering substances (*see* **Note 7**), it does not have to be buffer exchanged (*see* **Note 8**). In this case, prepare a solution of pure protein at a concentration of 20 μM in a volume of 100 μL in labeling buffer. Proceed to labeling **step 4**.
2. If the protein stock solution contains interfering substances (*see* also **Note 7**), perform buffer exchange to labeling buffer using the manufacturer's supplied spin column, buffer, and instructions (*see* **Note 9**). Resuspend the dried labeling buffer in 3 mL water. Prepare column A by resuspending the slurry. Remove excess storage solution by placing the column in a 1.5–2 mL microcentrifuge tube and centrifuging at 1500 *g* for 1 min. Wash the column three times with 300 μL labeling buffer.
3. Exchange the protein to labeling buffer by placing the protein solution in the center of the resin. Be careful not to disturb the resin. Place the column in a new microcentrifuge tube and centrifuge at 1500 *g* for 2 min.
4. Label the protein with the fluorescent dye. Dissolve the solid fluorescent dye by adding 30 μL DMSO (yielding a ~470 μM solution) and mixing thoroughly by vortexing (*see* **Note 10**). Prepare 100 μL 20–60 μM dye solution in labeling buffer. Add the dye to the protein from **steps 1** or **3** in a 1:1 volume ratio for a final 1:1–3:1 molar ratio of dye to protein in a 200 μL total volume (*see* **Note 11**). Incubate the reaction for 30 min at room temperature and in the dark (*see* **Note 12**). Proceed with **step 5** in the meantime.
5. Prepare the gravity flow column for purification of labeled protein and removal of unreacted dye (*see* **Note 13**). Pour off the storage solution from column B, and wash the column three times with 3 mL assay buffer (*see* also **Note 2**) in a 15 mL tube using the supplied adapter through gravity flow.
6. Separate the labeled protein obtained in **step 4** from unreacted dye. Apply the labeling reaction mixture to the center of column B from **step 5**. Let the sample enter the bed completely, and then add 300 μL assay buffer and discard the flow-through (*see* **Note 14**). Take the column out of the 15 mL tube. Add 600 μL assay buffer on top of the column and collect the eluate in ~50 μL fractions (one drop at a time) in appropriate tubes, e.g., 1.5 mL microcentrifuge tubes. Shield the fractions from light.
7. Verify the presence of labeled protein in the elution fractions by determining their fluorescence intensity and their capillary scan signal shape in the MST instrument (*see* Subheading 3.2). According to the gel filtration principle, larger particles will elute prior to smaller particles (*see* **Note 15**). At 20% LED

power, 10 nM labeled protein should yield fluorescence intensities of approximately 100–200 counts (*see* **Note 16** and Subheading 3.2).

8. Pool the fractions that contain labeled protein and shield them from light.
9. Determine the protein and dye concentrations, and derive the labeling efficiency by measuring the absorbance at 280 nm (A_{280}, for the protein) and 650 nm (A_{650}, for the dye) in a suitable spectrophotometer, e.g., a NanoDrop Spectrophotometer (Thermo Scientific), and applying the Lambert-Beer law (*see* **Note 17**). The molar absorbance of the dye at 650 nm is 250,000 M^{-1} cm^{-1}. Due to the absorption of the dye, the protein absorption at 280 nm has to be adjusted according to $A_{\text{protein}} = A_{280} – 0.028 \times A_{650}$.
10. Aliquot the labeled protein as 10 μL aliquots (e.g., into 200 μL PCR tubes), flash-freeze in liquid nitrogen, and store for several weeks to months at −80 °C (*see* **Note 18**).

3.1.2 DNA Preparation

1. Design a DNA sequence according to the requirements of the experiment. In this example, the DNA was obtained from a commercial supplier.
2. Design a second complementary DNA sequence, with the addition of a 5′ Cy5-label (*see* **Note 19**).
3. In the following steps, it is imperative that the samples are shielded from light (kept in the dark) as much as possible to prevent photobleaching.
4. Combine the single-stranded DNA sequences by mixing 10 nmol of each strand in a total volume of 100 μL (*see* **Note 20**).
5. Heat the sample to 95 °C, and let the DNA strands anneal by slowly returning to room temperature. This yields a 100 μM stock of fluorescent double-stranded DNA.
6. Test the integrity of the DNA by running it on a 1% agarose gel or, for very short polynucleotides, on a 5% polyacrylamide gel (*see* **Note 21**).

3.2 Optimization of Experimental Conditions

Optimization of experimental conditions is paramount to obtain high-quality data and derive accurate binding parameters. This is in particular due to the sensitivity of the MST experiment to protein adsorption to exposed surfaces and protein aggregation. To avoid such experimental artifacts, the correct capillary type has to be chosen, and the buffer composition needs to be optimized to ensure a homogeneous state of the sample, free from aggregation and sticking to surfaces. Here, we outline this procedure step-by-step for the fluorescent molecule (*see* Fig. 2). However, we note that some parameters are interrelated and that addition of the

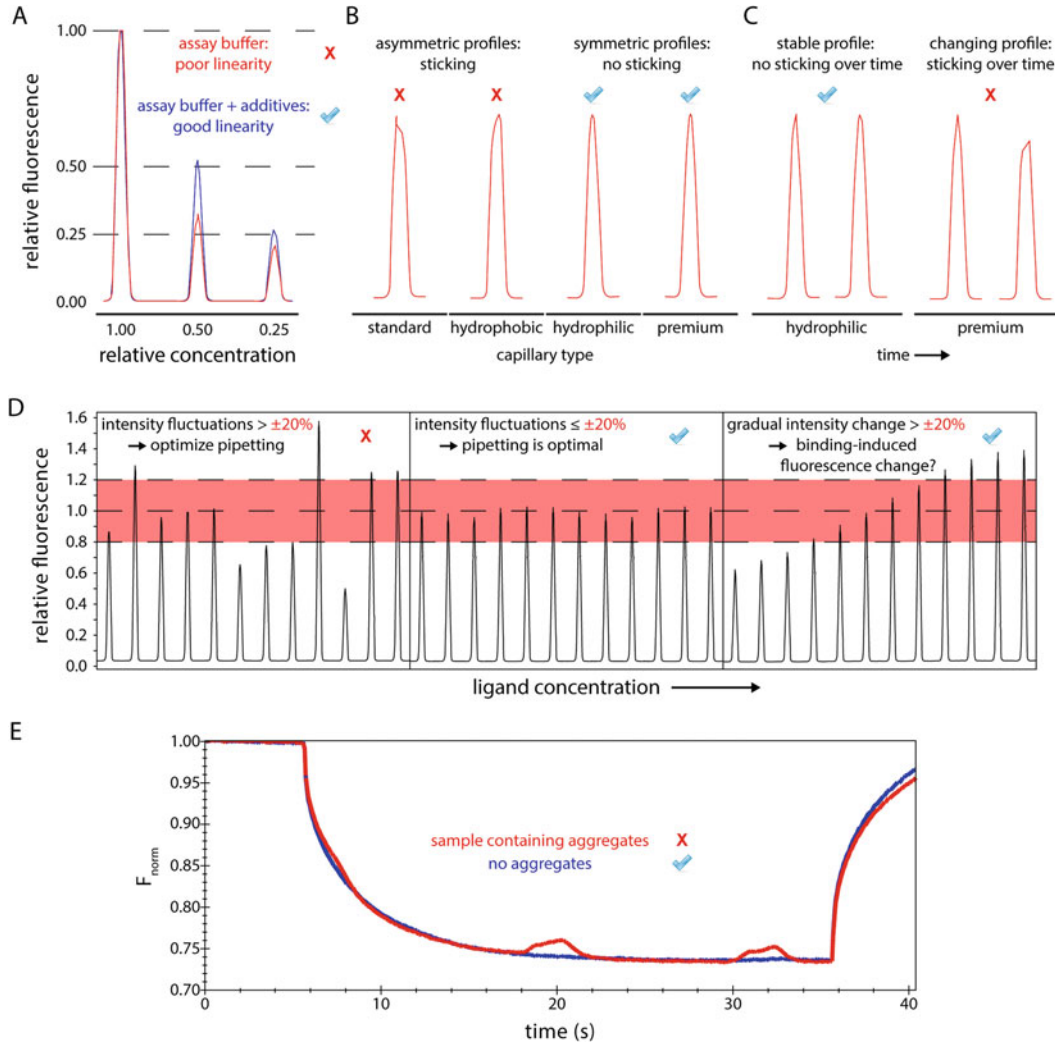

Fig. 2 Optimization of assay conditions. (**a**) Capillary scans of a dilution series of the fluorescently labeled molecule. The addition of additives (0.5 mg/mL BSA and 0.05% Tween-20) prevents sticking to reaction tubes and leads to a consistent dilution series. (**b**) Capillary scans of different types of capillaries loaded with the same labeled molecule. Asymmetric peaks are a sign of adsorption to the capillary wall. (**c**) Time-dependent changes in the capillary scans for the same molecule. While both premium and hydrophilic coatings show no adsorption initially, only hydrophilic capillaries remain free of adsorption over time. (**d**) Capillary scans of a titration series of the same molecule. Addition of 0.5 mg/mL BSA and 0.05% Tween-20 together with diligent pipetting improves the reproducibility of the fluorescence intensity to within the required limits (compare left and middle panel). Gradual fluorescence intensity changes are indicative of a binding reaction and can be used for analysis (*see* **Note 38**). (**e**) Aggregates in the sample led to irregularly shaped MST traces (red), which were prevented by spinning the sample for 20 min at 20,000 *g* and 4 °C to remove aggregates (blue) (*see* also **Note 29**). All data were acquired on NT-647-labeled $APLF^{AD}$ and its interaction with core histone complexes (*see* Subheading 3.6.2)

ligand may result in the need for further optimization. Hence, the procedure may need iteration and take a couple of hours and experimental trials.

1. Set the MST instrument to the desired reaction temperature, and wait for temperature equilibration. Keep the set temperature for the rest of the session (*see* **Notes 22** and **23**).
2. Make a calibration curve of the dye alone at the set temperature. Prepare 20 μL 200 nM dye solution in assay buffer in a capped, small-volume reaction tube to avoid evaporation (e.g., 200 μL PCR tubes), and label this tube 1. Label eight more PCR tubes 2 through 9. Add 10 μL assay buffer in each tube 2–9. Add 10 μL from tube 1 to 2 and mix five times by pipetting up and down. Then, add with a new pipette tip 10 μL from tube 2 to 3, and mix by pipetting five times up and down. Continue this series through to tube 9 (*see* **Note 24**). Fill all samples in standard capillaries (*see* **Note 25**), and perform a capillary scan (button "Start CapScan" in NT Control) at 50% LED power to measure the fluorescence intensity at each concentration. Prepare a calibration curve with fluorescence intensity on the *y*- and dye concentration on the *x*-axis.
3. Determine the optimal concentration of the fluorescently labeled molecule. Prepare a dilution series as in **step 2**, but using the stock of labeled molecule (protein or DNA) from Subheading 3.1. Fill the samples in standard capillaries, and start the capillary scan with 50% LED power. If the fluorescence is much lower than expected compared to the calibration curve or not linear over the dilution series, the fluorescent molecule likely sticks to the reaction tube or pipette tips (*see* also **step 4**). In that case, add 0.05% Tween-20 or another detergent (*see* Fig. 2a), and repeat the experiment. The measurement may also point out that there is sticking to the capillary (*see* **step 4**). If the sample behaves well, adjust the concentration to be lower or at most in the order of the expected K_D, while still resulting in a fluorescence signal with high signal-to-noise (*see* **Note 26**).
4. Determine the optimal type of capillary coating to ensure a homogenous sample. Load four capillaries of each type (Monolith NT standard, hydrophobic, hydrophilic (*see* **Note 3**), and premium treated) with working concentration of the labeled molecule determined in **step 3**, and perform a capillary scan. Inspect the shape of the fluorescence signal, which reflects the distribution of the labeled molecule in a cross section of the capillary. If a "U"- or "M"-shaped peak is observed instead of a smooth Gaussian-shaped fluorescence peak, the sample adsorbs to the capillary wall, which may be prevented using different capillary coatings (Fig. 2b). Also verify that no sticking occurs

over time by running a second capillary scan ~15 min after the first one (*see* Fig. 2c and **Note 27**). For further experiments, choose capillaries with minimal or no sticking. In case of sticking in all capillary types, proceed to **step 6**, and optimize the assay buffer.

5. Use the capillary profiles to also judge the reproducibility of the fluorescence intensity from the four replicates or from a binding experiment. Random intensity variations larger than 20% can be caused by inaccurate pipetting or sticking to the walls of reaction tubes and pipette tips (Fig. 2d). In that case, detergents like Tween-20, passivating agents like BSA, or higher salt concentrations in the assay buffer can be tested for improved results (*see* **Note 28**).
6. Check the thermophoresis signal for sample aggregation. Start a thermophoresis measurement with the following settings: labeled molecule at working concentration, LED power adjusted to yield at least 200 fluorescence counts, 40% MST power, and 30/5 s MST power on/off time. Aggregates, when present, will be transported in and out the measurement volume, causing sharp increases and decreases in fluorescence over time and a bumpy appearance of the MST curve (Fig. 2e). Make sure to use stocks and buffers that are free from aggregates or particulate matter, and adjust the assay buffer composition to prevent later aggregation (*see* **Note 29**).

3.3 Preparation of Dilution Series

To determine the dissociation constant (K_D) of a molecular interaction, a dilution series of up to 16 titration points is prepared (*see* **Notes 30** and **31**). The concentration of the fluorescent binding partner is kept constant, and the concentration of the unlabeled binding partner is varied (*see* **Notes 32** and **33**). Here, a twofold serial dilution is described, which is easily performed with minimum source for error, and results in optimally spaced data points along the sigmoidal binding curve.

1. Prepare 200 μL of the fluorescently labeled molecule (from Subheading 3.1) in the optimized buffer with double the concentration of the final reaction to account for the twofold dilution with titrant. Here, and in subsequent steps, use small-volume reaction tubes to avoid evaporation (e.g., 200 μL PCR tubes).
2. Prepare the titrant stock concentration to be 100-fold the expected K_D (*see* **Note 34**) in assay buffer (labeled tube 1) (*see* **Note 35**).
3. Prepare 15 tubes labeled 2 through 16 with 15 μL of the assay buffer. With a clean pipette tip, transfer 15 μL from tube 1 to tube 2, and mix well by pipetting five times up and down. Continue this serial dilution until tube 16 (*see* **Note 36**, *see* also **Note 24**).

4. Transfer 10 μL from tubes 1 to 16 to new reaction tubes, and add 10 μL of the fluorescently labeled sample stock from **step 1** to the tubes. Mix very well by pipetting five times up and down. After an adequate incubation time (at least 15 min, *see* **Note 37**), place the capillaries in the tubes to load the samples (*see* also **Note 25**).

3.4 MST Measurement

1. Load the capillaries of the previous step in the MST machine (*see* also **Note 23**), and perform a full MST measurement using the LED power setting determined in Subheading 3.2 and two consecutive measurements using 20% and 40% MST power (button "Start CapScan + MST Measurement"). The two measurements take ca. 20 min in total and can be followed in real time (*see* also **Note 27**).
2. Analyze the outcome of the measurements carefully to ensure the data is of sufficient quality. Inspect the results of the capillary scans to see if there is ligand-induced sticking; inspect the reproducibility of the fluorescence intensity to see if the variation is within a 20% margin (Fig. 2d, *see* **Note 38**); inspect the MST traces to see if there is ligand-induced aggregation (*see* Fig. 2e). If any of these issues are observed, carefully reevaluate the previous steps. A new round of assay condition optimization, this time including the ligand, can help to solve these issues. When no issues are encountered, proceed to **step 3**.
3. Analyze the MST-derived binding curve in the NT Affinity Analysis software. If a transition is observed, estimate its amplitude. Estimate the noise from the scatter in the data points at the lowest concentration of ligand where no binding is expected. Minimum amplitude should be 5 units (5‰ normalized fluorescence intensity change), and minimum signal-to-noise should be 3 (*see* **Note 39**). If either the amplitude or signal-to-noise is too low, increase the MST power to 60–80% (*see* **Notes 40** and **41**).
4. Once the final assay conditions have been established, perform the serial dilution (Subheading 3.3, **steps 3** and **4**) in triplicates, each time with two MST powers for the same dilution series.

3.5 MST Data Analysis

The manufacturer's NT Affinity Analysis software provides multiple options to extract a binding curve from the raw MST traces. The resulting binding curves can be fit directly in the software for a 1:1 binding model (*see* **Note 42**). The data can also be exported to be analyzed using third-party software. Here, we describe the default procedure using the instrument software, together with options for custom analysis. The use of custom software permits more realistic determination of errors in fit parameters and flexibility in choosing binding models.

1. In a new analysis set, click and drag the three replicates in a single experiment for a combined analysis.
2. If binding-induced changes in fluorescence intensity are observed, the binding curve can be directly derived and fit using the "Initial Fluorescence" button (*see* also **Note 38**). Otherwise, proceed to **step 3**.
3. Extract replicate-averaged binding curves using the two default settings: (*i*) "thermophoresis + T-jump" and (*ii*) "thermophoresis," and fit these using the thermodynamic model to extract the K_D. Compare the extracted values for consistency. If consistent, either setting can be used.
4. Use the "T-jump" method to see if there is temperature-related intensity change (TRIC) in the fluorescence, which may hold structural information if the location of the fluorophore is known.
5. Export the data for further analysis, error estimation of fit parameters, or fitting to custom binding models, e.g., using MATLAB, Python, or the PALMIST program of Scheuermann et al. [23].

3.6 Description of Examples

3.6.1 Different DNA Compaction Modes of HMfB

HMfB is an archaeal histone protein from *Methanothermus fervidus* with the ability to either bend or wrap DNA depending on the nucleotide sequence [24–26]. Here, we analyzed the HMfB-DNA interaction using two DNA sequences (78 bp each), either with a specific HMfB binding site ("specific sequence") or without ("nonspecific sequence"). Premium capillaries were used as reduced affinity was observed for the standard and hydrophobic capillaries, likely due to protein sticking to the capillaries. The F_{norm} values derived from the MST traces were normalized to obtain ΔF_{norm} values to facilitate comparison (Fig. 3a, b). Note that a custom dilution series was used to better sample the binding transitions (*see* **Note 43**).

For the nonspecific DNA sequence, a single binding transition is observed that can be fit to yield a K_D of 1 ± 0.2 μM (Fig. 3b). For the specific DNA sequence, two transitions are observed. The ΔF_{norm} decreases at low protein concentrations, indicating that the bound DNA is more mobile than the free DNA. At higher protein concentrations, however, the ΔF_{norm} increases indicating a less mobile, and possibly larger, protein-DNA complex. This second binding mode occurs at concentrations identical to those found for the nonspecific DNA, indicating that this is a nonspecific DNA binding mode. Together, this suggests that at high protein concentrations, HMfB forms the same structure independent of DNA sequence, while at low protein concentrations it forms a more compact structure at specific DNA sequences. This hypothesis is supported by data from complementary techniques (such as tethered particle motion (TPM) [27]) and is summarized in Fig. 3c.

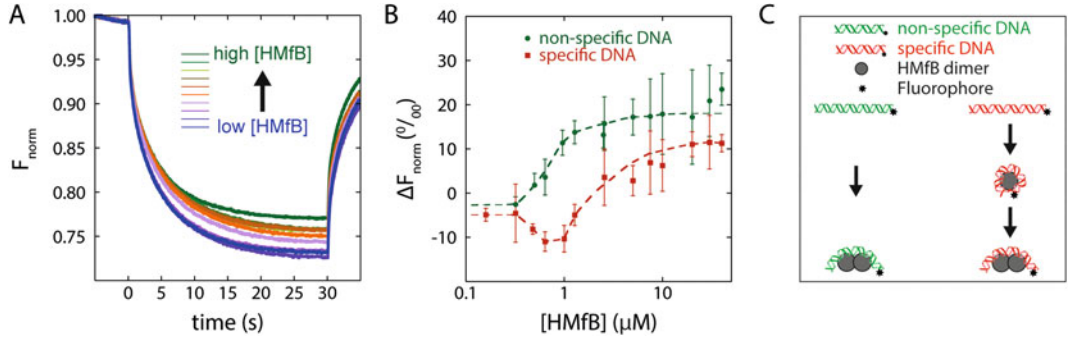

Fig. 3 MST analysis of HMfB interaction with two DNA substrates. (**a**) MST-thermophoresis curves for a range of HMfB concentrations. Data acquired at 22 °C, 40 nM of Cy5-labeled DNA in 50 mM Tris–HCl, pH 8.0, 75 mM KCl, premium capillaries, 20% laser power, 40% MST power. (**b**) Change in normalized fluorescence (ΔF_{norm}) for HMfB binding to a specific (red) or nonspecific (green) DNA sequence. Error bars indicate the standard deviation in a triplicate of experiments. (**c**) Model depicting the possible conformations of the HMfB-DNA complex. Without a specific binding site in the DNA substrate, HMfB binds as a multimer, forming a large structure. If a preferred DNA sequence is present, HMfB first forms a compact nucleosome-like structure. At higher HMfB concentrations, similar structures as seen for the nonspecific DNA sequence can be formed

3.6.2 Histone Binding by Histone Chaperone APLF

Histone chaperones are involved in the assembly and disassembly of the nucleosome for DNA replication, transcription, and repair [28]. Aprataxin and polynucleotide kinase-like factor (APLF) is a DNA repair protein with histone chaperone function [29]. Here, we studied the interaction of the APLF acidic domain ($APLF^{AD}$) with histone complexes using MST. $APLF^{AD}$ was labeled with the manufacturer's red dye NT-647-NHS according to Subheading 3.1.1. Given the low degree of labeling (DOL, ~15%) and the expected high affinity, 25 nM of $APLF^{AD}$ was used with 100% LED power to obtain an optimal fluorescence intensity of 400 counts. The assay buffer was supplemented with 0.5 mg/mL BSA and 0.05% Tween-20, and experiments were conducted in hydrophilic-treated capillaries to prevent sticking to the reaction tubes and the capillaries, respectively (*see* Fig. 2).

The MST data show that $APLF^{AD}$ binds with high and comparable affinities to both H2A-H2B and $(H3\text{-}H4)_2$, suggesting that APLF is a generic histone chaperone (Fig. 4). Interestingly, the binding curves show in both cases two transitions, suggesting two separate binding events (*see* **Note 43**), one with affinity in the higher nanomolar range and one in the micromolar range. The data were fit to a sequential-binding-site model using an in-house written MATLAB script (available upon request) with the Nelder-Mead simplex algorithm as minimization procedure. Errors in the best-fit parameters represent the 95% confidence interval based on statistical F-tests [23]. The additional binding mode of histones to $APLF^{AD}$ may be relevant for its chaperoning mechanism, promoting the retention of multiple copies of histone complexes for nucleosome assembly at DNA repair sites [30, 31].

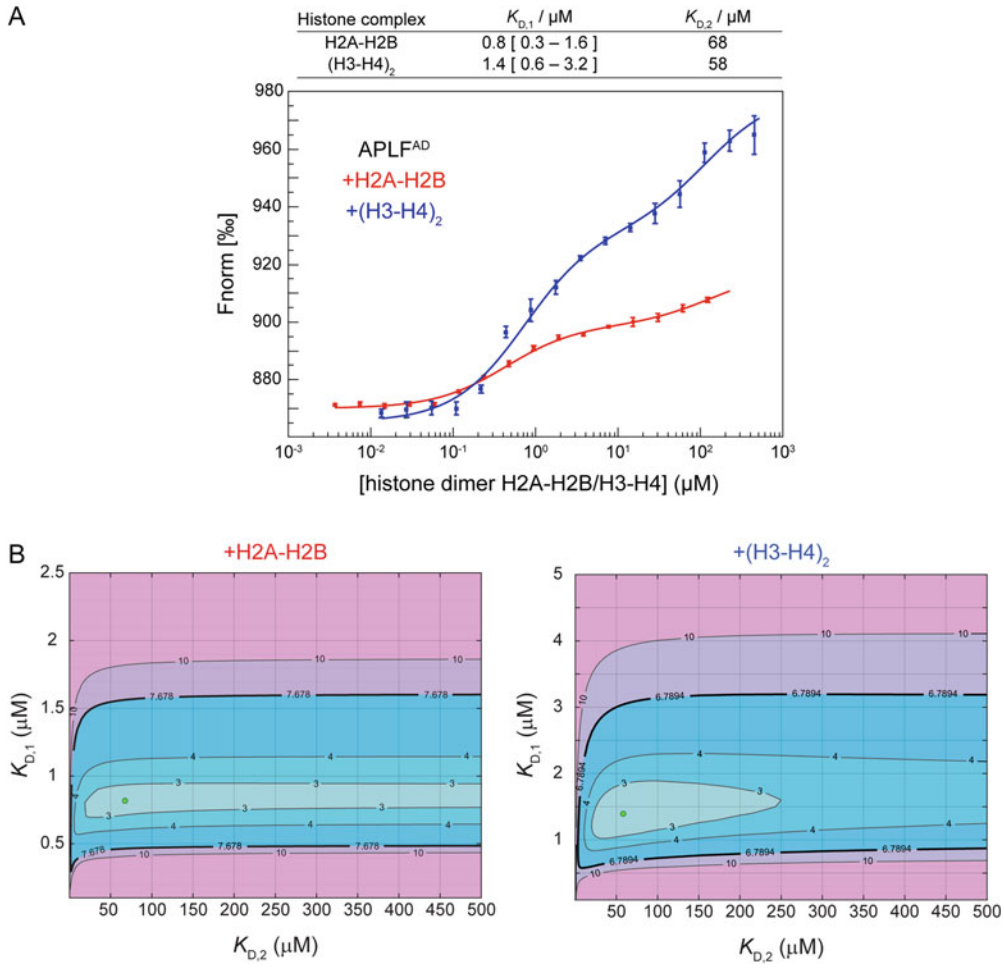

Fig. 4 APLF^{AD} binds with similar affinities to H2A–H2B and (H3–H4)$_2$. (**a**) MST binding curves of H2A–H2B (red) or (H3–H4)$_2$ (blue) with fluorescently labeled APLF^{AD} (25 nM) in assay buffer (25 mM NaPi, pH 7.0, 300 mM NaCl, supplemented with 0.5 mg/mL BSA and 0.05% Tween-20), recorded at 25 °C, 20% MST power, 100% LED power, with 30/5 s laser-on/off time. The binding curve represents the average from three measurements with standard deviation. Best-fit values for the corresponding affinities and 95% confidence limits are listed in the table. (**b**) Plots showing the reduced χ^2-surface that expresses the quality of the fit in contour mode as function of the high-affinity ($K_{D,1}$) and the low-affinity ($K_{D,2}$) dissociation constants for H2A–H2B (left) and (H3–H4)$_2$ (right) binding to APLF^{AD}. The best-fit values are indicated by a green dot. The 95% confidence critical value for the reduced χ^2 is indicated with a thick black line. (Figure reproduced from Ref. [31] with permission from the authors)

3.6.3 Binding of a Nucleosome-Mimicking Peptide to a Reader Protein

Posttranslational histone modifications are key regulators of chromatin function, mostly through their specific interaction with so-called reader proteins. We recently found that the recognition of trimethylated lysine 36 on histone H3 (H3K36me3) by the PSIP1-PWWP domain is driven by the nucleosomal context of this modification [32]. PSIP1-PWWP binds with very low affinity ($K_D = 17$ mM) to an H3K36me3 peptide, but with 10,000-fold

enhanced affinity to modified nucleosomes [32]. Here, we address the importance of electrostatics by using MST to investigate the binding of PSIP1-PWWP to an $H3K_C36me3$ peptide decorated with a stretch of glutamate residues ($H3K_C36me3\text{-}E_7$) that mimic the nucleosomal DNA. NanoTemper dye NT-647-MALEIMIDE was coupled to a cysteine mutant of PSIP1-PWWP(N86C). Premium capillaries and 0.05% Tween-20 were used to avoid fluorescence loss due to sticking of the protein.

The capillary scan of the titration series showed a ligand-dependent decrease in initial fluorescence only for the trimethylated version of the peptide and not for an unmodified peptide (Fig. 5a). Additionally, a denaturing test (*see* also **Note 38**) showed full fluorescence recovery (data not shown), proving that the changes are binding induced. Fits of the "initial fluorescence," "T-jump," and "thermophoresis + T-jump" all give comparable and consistent K_D values of ~1.6 mM (Fig. 5b–d). The tenfold increase in binding affinity compared to the native H3K36me3 peptide underscores the importance of the nucleosomal context, in which both electrostatic and geometric factors are critical [33].

3.6.4 Analysis of a Nucleosome-Peptide Interaction

The latency-associated nuclear antigen (LANA) of Kaposi's sarcoma-associated herpes virus (KHSV) binds to nucleosomes to ensure the persistence of the KHSV cosmid in both daughter cells during host cell division [34]. A short peptide sequence from LANA binds strongly and specifically to the acidic patch on the H2A-H2B surface of the nucleosome [35]. Here, we analyzed the binding of a peptide containing residues 2–22 of LANA (2.1 kDa) to nucleosomes (210 kDa) that were labeled using NanoTemper's NT-647-Red-NHS dye after reconstitution [36]. Degree of labeling (DOL) was in the order of 10%, sufficient to yield 600 fluorescence counts with a 135 nM solution and 100% LED power. Labeling and purification did not interfere with nucleosome integrity as shown by native PAGE analysis (data not shown). Optimization of the conditions led to the choice of 0.1 mg/mL BSA as additive—0.01% Triton X-100 or 0.01% Tween-20 resulted in comparatively weaker thermophoretic changes upon LANA binding (Fig. 6a). Hydrophobic capillaries were selected to prevent binding-induced sticking.

The MST binding curves show a clear transition that was fit using an in-house written MATLAB script (available upon request) to a single binding event with a K_D of 0.16 μM, which agrees well with the previously published value of 0.24 μM under slightly different conditions [37] (Fig. 6b). These data demonstrate the possibility to reliably determine binding parameters of small-molecule effectors to fluorescently labeled nucleosomes. While the thermophoretic changes may be larger using the reverse labeling setup, the current strategy allows screening of several effectors with minimum nucleosome consumption.

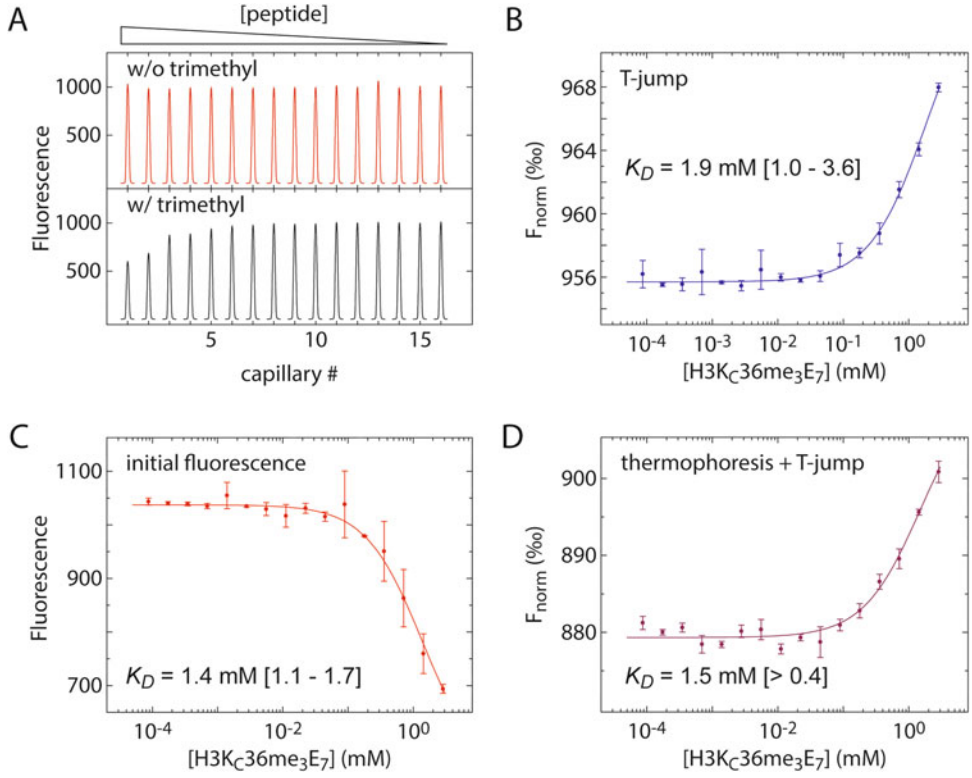

Fig. 5 MST of nucleosome-mimicking H3K$_C$36me3 peptides binding to the PSIP1-PWWP domain. (**a**) Capillary scans for H3K$_C$36-E$_7$ peptides (SAPATGGVCKEEEEEEE) with (red) and without (black) cysteine-based trimethyl lysine analogue [41]. (**b**, **c**, **d**) Analysis of the MST measurements was done by fitting the data for "T-jump" (**b**), "initial fluorescence" (**c**), and "thermophoresis + T-jump" (**d**). Best-fit values for the K_D and 95% confidence limits are indicated in the plots. Data recorded on 0.35 μM NT-647-labeled PWWP(N86C) domain titrated with peptide in 10 mM Tris–HCl, pH 7.5, 100 mM KCl, supplemented with 0.05% Tween-20, 25 °C, 20%/20% LED/MST power, with 30/5 s laser-on/off time

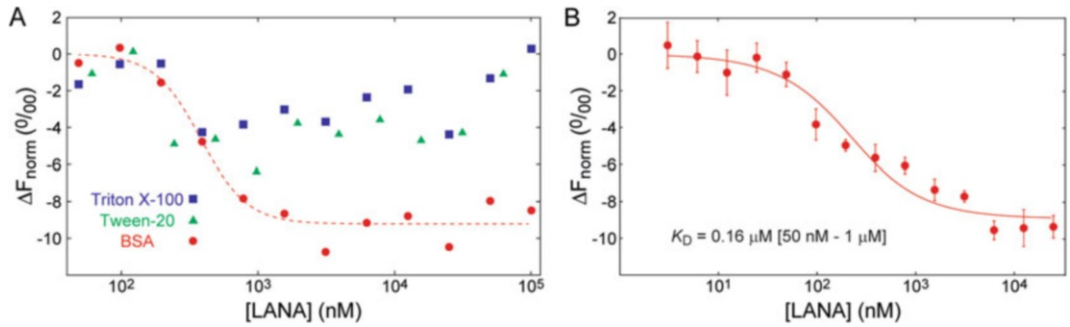

Fig. 6 MST of LANA binding to mononucleosomes. (**a**) Buffer optimization: comparison of the binding curves of 200 nM NT-647-labeled nucleosomes titrated with LANA in 10 mM Tris–HCl, pH 7.5, 100 mM KCl, supplemented with either BSA, Tween-20, or Triton X-100. A fit to the BSA curve is shown to guide the view. (**b**) MST binding curve (average of three independent measurements, with standard deviations) of 135 nM of NT-647-labeled mononucleosomes titrated with LANA. Measurements were performed at 22 °C, 50% MST, and 100% LED power with 30/5 s laser-on/off time. Best-fit values and 95% confidence intervals are shown in the figure

4 Notes

1. A more sensitive second generation of the dyes used in this study is available. Furthermore, non-covalent labeling of the commonly used His-tag for protein purification is also possible. However, one is by no means restricted to using the manufacturer's fluorescent labeling kits. There are many commercially available fluorescent compounds that can be coupled to free amino or thiol groups. Make sure to use fluorophores compatible with the excitation and detection wavelengths of your MST instrument.
2. "Assay buffer" here refers to the buffer of choice in which the interaction is investigated. The molecules should be stable and well behaved in this buffer. Typical buffer conditions are 50 mM Tris–HCl, pH 7.4, 150 mM NaCl, 10 mM $MgCl_2$, 0.05% Tween-20.
3. Hydrophilic- and hydrophobic-treated capillaries are no longer available. Premium capillaries are advised as replacement.
4. Prepare all solutions using water (resistivity 18.2 MΩ × cm and organic content less than five parts per billion) and analytical-grade reagents.
5. Higher stock concentrations are useful to have most flexibility for adjusting concentrations and exact assay buffer composition during optimization of the experimental conditions (*see* Subheading 3.2) or in follow-up experiments.
6. In case no binding is detected with one binding partner fluorescently labeled, it can be tried to invert the experimental setup and label the other binding partner. Alternatively, a different fluorescence labeling strategy can be used, e.g., using different chemistry (NHS-ester vs. maleimide), or non-covalent labeling of a His-tag.
7. Primary amines are present in, e.g., Tris buffer, glycine, ethanolamine, and glutathione (GSH). Sulfhydryls are present in, e.g., reducing agents dithiothreitol (DTT), β-mercaptoethanol (BME), and GSH. These substances can interfere with the NHS and maleimide labeling. Tris(2-carboxyethyl)phosphine (TCEP) can be used as reducing agent during labeling. However, at mM concentrations, TCEP can covalently attach to some red dyes and quench them. Hence, it must be used at low concentrations or replaced with DTT for the binding assay. Samples for labeling should not contain protein impurities or carriers like bovine serum albumin (BSA).
8. Buffer exchange to labeling buffer (**steps 2** and **3**) can be skipped if the protein is purified directly in a suitable buffer (good buffers are HEPES, PBS, and Na-Ac with $6.5 < \text{pH} < 8.5$).

9. If a labeling buffer is used other than the one supplied, a higher excess of dye might be required for sufficient degree of labeling (DOL).
10. The dye can be used for a few hours after resuspending it according to the manufacturer's manual. For longer storage of stock solutions, dye may be frozen and aliquoted in DMSO under anhydrous conditions to prevent hydrolysis.
11. For some samples, degree of labeling (DOL) may be increased by using a higher-fold excess of dye.
12. The reaction can be carried out in a drawer or cupboard, or the reaction tube can be wrapped in aluminum foil.
13. Unreacted dye is a source of unwanted fluorescence noise that will be detected along with the wanted fluorescence signal from the labeled protein. Hence, for optimal signal-to-noise and best MST results, unreacted dye needs to be removed.
14. When doing a 200 μL labeling reaction, the volume must be adjusted to 500 μL after the sample has entered the column bed by adding 300 μL assay buffer on top. If a scale-up or scale-down of the reaction is necessary, make sure the total volume loaded on the column is 500 μL. Ensure the whole labeling mix has entered the column bed before completing to 500 μL.
15. Use the early fractions that contain higher amounts of labeled protein. Depending on the assay buffer composition, later fractions might contain unreacted dye. It can also be helpful to check the thermophoresis signal for bumps which are indicative of aggregates in the sample (*see* Fig. 2e).
16. If required, after fluorescent labeling, the protein can be concentrated using a device like an Amicon Ultra-0.5 centrifugal filter unit (Millipore).
17. Typically, the degree of labeling (DOL) is between 0.5 and 1.1 (according to the manufacturer).
18. If the stored protein is to be used for a new interaction study, repetition of previous experiments can be conducted to assess the stability and quality of the sample.
19. It is possible to generate much larger labeled DNA sequences for MST using polymerase chain reaction (PCR) and fluorescently labeled DNA primers [27, 38].
20. You can make the DNA stock at any concentration. If you choose to make a lower concentration stock, it is imperative that the two DNA strands are mixed in a 1:1 molar ratio. Making a higher concentration stock allows you to reduce the effects of incidental photobleaching. Furthermore, the Monolith NT anti-photobleach kit can be used to eliminate fluorophore photobleaching caused by reactive oxygen species during fluorescence excitation of very low concentrated target solutions that are usually required for high-affinity interactions.

21. If you do not observe a single band for your double-stranded DNA in your control step, you should redo the annealing of the two strands with a lower temperature decrease rate, thereby reducing the rate at which the two DNA strands anneal.
22. The experimental temperature in the MST instrument can be set between 22 and 45 °C or left unspecified for room temperature. The temperature is best set to a defined value, ideally above room temperature, and reported together with the used MST power.
23. After opening of the instrument's door for sample insertion, close the door, and wait until the set temperature is reached as shown on the instrument's display.
24. Change the pipette tip after each transfer, or, alternatively, pre-wet the tip before the first transfer, and use it for the subsequent transfers. For some pipettes, it may be necessary to slightly reset the pipetting volume after placing a new pipette tip. Importantly, perform each pipetting step consistently in the same way to avoid pipetting errors.
25. The capillaries take up to 10 μL of liquid. The tube and capillary can be tilted to ease filling. To have air on both sides, the capillary can be inverted for 1 or 2 s after loading.
26. Typically, 5–100 nM of fluorescently labeled molecule is sufficient to obtain optimal fluorescence, with intensity above 400 and below 2000, with a minimum of 200. The LED power can be varied between 15% and 95% to achieve this. For very high-affinity interactions, use the lowest possible concentration in which you get 200 fluorescence counts with 95% LED power.
27. Capillary scans of each new titration should be performed at the start of the experiment to assess the quality of the samples and again at the end of the experiment to check for changes in the fluorescence peak shape and intensity that can occur over time.
28. Additives should be used at the lowest functional concentration possible as they may interfere with the binding at too high concentrations. The NanoTemper buffer exploration kit can be used to find suitable assay buffers.
29. Aggregates can be removed by centrifuging sample stocks (20 min, 20,000 *g*, 4 °C, or using an Ultrafree-MC or Ultrafree-CL centrifugal filter unit (Millipore)) and filtering buffers through 0.22 μm filters. Detergents such as Tween-20 or Triton X-100 (0.01–0.1%) or changes in assay buffer conditions (different ionic strength, pH) can also help to prevent aggregation or binding-induced aggregation.
30. Do not use less than 10 titration points per experiment because that will lead to inaccuracy in the determined K_D.

31. A control experiment can be conducted with an unrelated nonbinding molecule or a binding-deficient mutant of the binding partner.
32. If the concentration of labeled molecule is on the order of the K_D, the dilution series (Subheading 3.3) is best prepared linearly to optimally sample the binding curve, in which case the data is best plotted using a linear *x*-axis resulting in a hyperbole binding curve.
33. The "Concentration Finder" tool within the NT Control software can be used to simulate binding curves and determine the required titrant concentration ranges. In case the dissociation constant is unknown, a three- to fivefold dilution series starting from a high concentration will allow monitoring of binding events within a wide ligand concentration range. If a binding transition is observed, the titrant stock concentration and dilution series can be adjusted accordingly.
34. As in any quantitative essay, it is essential to accurately determine protein concentrations, to work with calibrated pipettes, and to perform precise and reproducible protein dilutions. In contrast to the fluorescent target, the ligand concentration needs to be known precisely since concentration inaccuracy alters the derived K_D.
35. Serial dilution of ligand in assay buffer should not introduce any changes in buffer composition except the ligand concentration. Working with fluorescent target and ligand molecules originating from different buffer stocks is no problem. For compounds in organic solvents (e.g., DMSO), the dilution series can be prepared in the solvent and then added to the fluorescent target with a low final organic solvent concentration.
36. After having obtained practical experience and confidence with the pipetting procedure, the pipetting volumes can be reduced to half to save material.
37. The incubation time is necessary to establish equilibrium which is determined by the binding kinetics of complex formation (association and dissociation kinetics). In sporadic cases with very high affinity and very low dissociation rates, equilibration may take hours to days [23]. Equilibration can be verified by repeating a titration series after different incubation times, e.g., 15, 30, and 60 min.
38. A systematic ligand-dependent increase or decrease of fluorescence intensity may be caused by binding if the fluorophore is close to the binding site. To determine if this is the case, spin down the reaction tubes for 10 min at 15,000 *g* and 4 °C, remove 10 μL of supernatant, and add this to 10 μL of denaturing buffer (40 mM DTT + 4% sodium dodecyl sulfate (SDS)

or 7 M urea if the assay buffer contains potassium that would precipitate SDS), and then heat for 5 min at 95 °C, load the samples into capillaries, and perform a capillary scan. If the fluorescence intensity is now constant within 20%, the effect was binding-induced. If the effect remains, sample was lost due to sticking or aggregation and a new round of optimization has to be started.

39. Compare Refs. [23, 39, 40] for MST curves with a range of signal-to-noise ratios.
40. Reduce the laser-on time at high MST powers to 10 s to reduce effects from sample heating.
41. Sign and amplitude of the thermophoresis signal are typically not analyzed since they depend in a complex manner on the changes in conformation, size, charge, and hydration of the molecule.
42. Avoid the use of the Hill equation since the reported EC50 values are protein concentration dependent and the fit cooperativity coefficient may be larger than the number of binding sites. Use the Hill fit only when the investigated interaction is known to be cooperative.
43. In case multiple binding transitions are observed in an MST titration, it can be useful to confirm the result with complementary techniques and to find out the origin of the effect (either multiple ligand binding sites on the target or concentration-dependent multimerization of the ligand).

Acknowledgments

We thank the NanoTemper team for their support and advice. We thank Prof. Dr. G.A. van der Marel and N. Meeuwenoord (Leiden University) for support in peptide synthesis and purification. This work was supported by the Netherlands Organization for Scientific Research (NWO) (VIDI 864.08.001, VICI 016.160.613 to RTD and VIDI 723.013.010 to HvI) and NanonextNL of the government of the Netherlands and 130 partners.

References

1. Flores KJ, Kariawasam R, Gimenez XA, Helder S, Cubeddu L, Gamsjaeger R, Ataide FS (2015) Biophysical characterisation and quantification of nucleic acid-protein interactions: EMSA, MST and SPR. Curr Protein Pept Sci 16:727–734. https://doi.org/10.2174/1389203716666150505230806
2. Oda M, Nakamura H (2000) Thermodynamic and kinetic analyses for understanding sequence-specific DNA recognition. Genes Cells 5:319–326. https://doi.org/10.1046/j.1365-2443.2000.00335.x
3. van Emmerik CL, van Ingen H (2019) Unspinning chromatin: revealing the dynamic nucleosome landscape by NMR. Prog Nucl Magn Reson Spectrosc 110:1–19. https://doi.org/10.1016/j.pnmrs.2019.01.002
4. Ludwig C (1856) Diffusion zwischen ungleich erwärmten Orten gleich zusammengesetzter

Lösung. Sitzungsber Akad Wiss Wien Math-Naturwiss 20:539

5. Wienken CJ, Baaske P, Rothbauer U, Braun D, Duhr S (2010) Protein-binding assays in biological liquids using microscale thermophoresis. Nat Commun 1:100. https://doi.org/10.1038/ncomms1093
6. Romain M, Thiroux B, Tardy M, Quesnel B, Thuru X (2020) Measurement of protein-protein interactions through microscale thermophoresis (MST). Bio Protoc 10:e3574. https://doi.org/10.21769/BioProtoc.3574
7. Seidel SA, Wienken CJ, Geissler S, Jerabek-Willemsen M, Duhr S, Reiter A, Trauner D, Braun D, Baaske P (2012) Label-free microscale thermophoresis discriminates sites and affinity of protein-ligand binding. Angew Chem Int Ed Eng 51:10656–10659. https://doi.org/10.1002/anie.201204268
8. Duhr S, Braun D (2006) Why molecules move along a temperature gradient. Proc Natl Acad Sci USA 103:19678–19682. https://doi.org/10.1073/pnas.0603873103
9. Seidel SA, Dijkman PM, Lea WA, van den Bogaart G, Jerabek-Willemsen M, Lazic A, Joseph JS, Srinivasan P, Baaske P, Simeonov A, Katritch I, Melo FA, Ladbury JE, Schreiber G, Watts A, Braun D, Duhr S (2013) Microscale thermophoresis quantifies biomolecular interactions under previously challenging conditions. Methods 59:301–315. https://doi.org/10.1016/j.ymeth.2012.12.005
10. Bartoschik T, Galinec S, Kleusch C, Walkiewicz K, Breitsprecher D, Weigert S, Muller YA, You C, Piehler J, Vercruysse T, Daelemans D, Tschammer N (2018) Near-native, site-specific and purification-free protein labeling for quantitative protein interaction analysis by MicroScale Thermophoresis. Sci Rep 8:4977. https://doi.org/10.1038/s41598-018-23154-3
11. Jerabek-Willemsen M, André T, Wanner R, Roth HM, Duhr S, Baaske P, Breitsprecher D (2014) MicroScale Thermophoresis: interaction analysis and beyond. J Mol Struct 1077:101–113. https://doi.org/10.1016/j.molstruc.2014.03.009
12. Schubert T, Pusch MC, Diermeier S, Benes V, Kremmer E, Imhof A, Langst G (2012) Df31 protein and snoRNAs maintain accessible higher-order structures of chromatin. Mol Cell 48:434–444. https://doi.org/10.1016/j.molcel.2012.08.021
13. Zillner K, Filarsky M, Rachow K, Weinberger M, Langst G, Nemeth A (2013) Large-scale organization of ribosomal DNA chromatin is regulated by Tip5. Nucleic Acids Res 41:5251–5262. https://doi.org/10.1093/nar/gkt218
14. Su XC, Wang Y, Yagi H, Shishmarev D, Mason CE, Smith PJ, Vandevenne M, Dixon NE, Otting G (2014) Bound or free: interaction of the C-terminal domain of Escherichia coli single-stranded DNA-binding protein (SSB) with the tetrameric core of SSB. Biochemistry 53:1925–1934. https://doi.org/10.1021/bi5001867
15. Silva AP, Ryan DP, Galanty Y, Low JK, Vandevenne M, Jackson SP, Mackay JP (2016) The N-terminal region of chromodomain helicase DNA-binding protein 4 (CHD4) is essential for activity and contains a high mobility group (HMG) box-like-domain that can bind poly(ADP-ribose). J Biol Chem 291:924–938. https://doi.org/10.1074/jbc.M115.683227
16. Yamagata K, Kobayashi A (2017) The cysteine-rich domain of TET2 binds preferentially to mono- and dimethylated histone H3K36. J Biochem 161:327–330. https://doi.org/10.1093/jb/mvx004
17. Zillner K, Jerabek-Willemsen M, Duhr S, Braun D, Langst G, Baaske P (2012) Microscale thermophoresis as a sensitive method to quantify protein: nucleic acid interactions in solution. Methods Mol Biol 815:241–252. https://doi.org/10.1007/978-1-61779-424-7_18
18. Zhang W, Duhr S, Baaske P, Laue E (2014) Microscale thermophoresis for the assessment of nuclear protein-binding affinities. Methods Mol Biol 1094:269–276. https://doi.org/10.1007/978-1-62703-706-8_21
19. Schubert T, Längst G (2015) Studying epigenetic interactions using MicroScale Thermophoresis (MST). AIMS Biophys 2:370–380. https://doi.org/10.3934/biophy.2015.3.370
20. Willhoft O, McCormack EA, Aramayo RJ, Bythell-Douglas R, Ocloo L, Zhang X, Wigley DB (2017) Crosstalk within a functional INO80 complex dimer regulates nucleosome sliding. elife 6:e25782. https://doi.org/10.7554/eLife.25782
21. Schrader A, Gross T, Thalhammer V, Langst G (2015) Characterization of Dnmt1 binding and DNA methylation on nucleosomes and nucleosomal arrays. PLoS One 10:e0140076. https://doi.org/10.1371/journal.pone.0140076
22. Zocco M, Marasovic M, Pisacane P, Bilokapic S, Halic M (2016) The Chp1 chromodomain binds the H3K9me tail and the nucleosome core to assemble heterochromatin. Cell Discov 2:16004. https://doi.org/10.1038/celldisc.2016.4

23. Scheuermann TH, Padrick SB, Gardner KH, Brautigam CA (2016) On the acquisition and analysis of microscale thermophoresis data. Anal Biochem 496:79–93. https://doi.org/10.1016/j.ab.2015.12.013
24. Bailey KA, Marc F, Sandman K, Reeve JN (2002) Both DNA and histone fold sequences contribute to archaeal nucleosome stability. J Biol Chem 277:9293–9301. https://doi.org/10.1074/jbc.M110029200
25. Henneman B, Dame RT (2015) Archaeal histones: dynamic and versatile genome architects. AIMS Microbiol 1:72–81. https://doi.org/10.3934/microbiol.2015.1.72
26. Erkelens AM, Henneman B, van der Valk RA, Kirolos NCS, Dame RT (2023) Specific DNA binding of archaeal histones HMfA and HMfB. Front Microbiol 14:1166608. https://doi.org/10.3389/fmicb.2023.1166608
27. Henneman B, Heinsman J, Battjes J, Dame RT (2018) Quantitation of DNA-binding affinity using tethered particle motion. Methods Mol Biol 1837:257–275. https://doi.org/10.1007/978-1-4939-8675-0_14
28. Hammond CM, Stromme CB, Huang H, Patel DJ, Groth A (2017) Histone chaperone networks shaping chromatin function. Nat Rev Mol Cell Biol 18:141–158. https://doi.org/10.1038/nrm.2016.159
29. Mehrotra PV, Ahel D, Ryan DP, Weston R, Wiechens N, Kraehenbuehl R, Owen-Hughes-T, Ahel I (2011) DNA repair factor APLF is a histone chaperone. Mol Cell 41:46–55. https://doi.org/10.1016/j.molcel.2010.12.008
30. Corbeski I, Guo X, Eckhardt BV, Fasci D, Wiegant W, Graewert MA, Vreeken K, Wienk H, Svergun DI, Heck AJR, van Attikum H, Boelens R, Sixma TK, Mattiroli F, van Ingen H (2022) Chaperoning of the histone octamer by the acidic domain of DNA repair factor APLF. Sci Adv 8:eabo0517. https://doi.org/10.1126/sciadv.abo0517
31. Corbeski I, Dolinar K, Wienk H, Boelens R, van Ingen H (2018) DNA repair factor APLF acts as a H2A-H2B histone chaperone through binding its DNA interaction surface. Nucleic Acids Res 46:7138–7152. https://doi.org/10.1093/nar/gky507
32. van Nuland R, van Schaik FMA, Simonis M, van Heesch S, Cuppen E, Boelens R, Timmers HTM, van Ingen H (2013) Nucleosomal DNA binding drives the recognition of H3K36-methylated nucleosomes by the PSIP1-PWWP domain. Epigenetics Chromatin 6:12. https://doi.org/10.1186/1756-8935-6-12
33. Horn V, Jongkees SAK, van Ingen H (2020) Mimicking the nucleosomal context in peptide-based binders of a H3K36me reader increases binding affinity while altering the binding mode. Molecules 25:4951. https://doi.org/10.3390/molecules25214951
34. Ballestas ME, Chatis PA, Kaye KM (1999) Efficient persistence of extrachromosomal KSHV DNA mediated by latency-associated nuclear antigen. Science 284:641–644. https://doi.org/10.1126/science.284.5414.641
35. Barbera AJ, Chodaparambil JV, Kelley-Clarke-B, Joukov V, Walter JC, Luger K, Kaye KM (2006) The nucleosomal surface as a docking station for Kaposi's sarcoma herpesvirus LANA. Science 311:856–861. https://doi.org/10.1126/science.1120541
36. Dyer PN, Edayathumangalam RS, White CL, Bao Y, Chakravarthy S, Muthurajan UM, Luger K (2004) Reconstitution of nucleosome core particles from recombinant histones and DNA. Methods Enzymol 375:23–44. https://doi.org/10.1016/s0076-6879(03)75002-2
37. Beauchemin C, Moerke NJ, Faloon P, Kaye KM (2014) Assay development and high-throughput screening for inhibitors of Kaposi's sarcoma-associated herpesvirus N-terminal latency-associated nuclear antigen binding to nucleosomes. J Biomol Screen 19:947–958. https://doi.org/10.1177/1087057114520973
38. van der Valk RA, Qin L, Moolenaar GF, Dame RT (2018) Quantitative determination of DNA bridging efficiency of chromatin proteins. Methods Mol Biol 1837:199–209. https://doi.org/10.1007/978-1-4939-8675-0_12
39. Allam R, Scherbaum CR, Darisipudi MN, Mulay SR, Hagele H, Lichtnekert J, Hagemann JH, Rupanagudi KV, Ryu M, Schwarzenberger C, Hohenstein B, Hugo C, Uhl B, Reichel CA, Krombach F, Monestier M, Liapis H, Moreth K, Schaefer L, Anders HJ (2012) Histones from dying renal cells aggravate kidney injury via TLR2 and TLR4. J Am Soc Nephrol 23:1375–1388. https://doi.org/10.1681/ASN.2011111077
40. van der Berg JP, Madoori PK, Komarudin AG, Thunnissen AM, Driessen AJ (2015) Binding of the lactococcal drug dependent transcriptional regulator LmrR to its ligands and responsive promoter regions. PLoS One 10:e0135467. https://doi.org/10.1371/journal.pone.0135467
41. Simon MD, Chu F, Racki LR, de la Cruz CC, Burlingame AL, Panning B, Narlikar GJ, Shokat KM (2007) The site-specific installation of methyl-lysine analogs into recombinant histones. Cell 128:1003–1012. https://doi.org/10.1016/j.cell.2006.12.041